

PACS numbers: 42.65.Hw
DOI: 10.1070/QE2003v033n01ABEH002367

Four-wave interactions in an active XeCl plasma

Yu.K. Verevkin, E.Ya. Daume, V.N. Petryakov

***Abstract*. A problem of the four-wave interaction of radiation in a three-level medium, where the lower working level is a repulsive one, is solved. This situation is characteristic of UV-active excimer molecules. The solution to this problem is compared to the results obtained for a two-level model. The coefficient of reflection into a conjugate wave is measured as a function of the small-signal gain in an active XeCl excimer plasma. An influence of the four-wave interaction on the characteristics of optical amplifiers and master oscillators operating with narrow-band radiation is observed.**

Keywords: *three-level model, nondegenerate interaction of counter-propagating waves, reflection efficiency of the probe radiation.*

1. Introduction

Four-wave interactions in resonance media are of interest for spectroscopy and optimisation of high-power laser systems [1 – 6]. For the purpose of spectroscopy, it is sufficient to solve this problem in the approximation of expansion of the polarisation at the frequencies of strong waves in powers of the saturating field. In this case, the population difference must be close to an equilibrium value [1, 2]. In order to optimise laser systems, it is necessary to solve the problem of the influence of the strong-wave amplitudes on the character of resonance-medium saturation as exactly as possible [7]. In the first case, the problems of wave interaction have been solved for both the two-level and multilevel models. Note that, in many works and spectroscopic problems, strong fields are exactly taken into account in the first-order solution in terms of a weak field. Using such an approach, a number of interesting effects, such as line broadening and the appearance of several peaks, which depend on the interaction coefficient of the waves and their frequencies and intensities, have been revealed [8, 9].

In the second case, degenerate and nondegenerate four-wave interactions were considered theoretically in a two-level resonance medium [3, 4, 6, 7], where the frequencies of two (strong) waves were assumed equal (ω_1). Upon the nondegenerate interaction, the frequency ω_3, amplitude, and propagation direction of the third (weak) wave are also specified, and the conditions for the appearance of the fourth wave with a frequency $\omega_4 = 2\omega_1 - \omega_3$ are analysed. However, the lower working state of UV-active excimer molecules (XeF, XeCl, etc.) is repulsive or weakly bound [10]; therefore, it is interesting to elucidate the effect of this feature on four-wave interactions. This feature can be described in the simplest form within the framework of a three-level model.

In this paper, we extend the problem of four-wave interaction to the case of a three-level medium taking into account changes in the amplitudes of strong waves.

V.I. Verevkin, E.Ya. Daume, V.N. Petryakov Institute of Applied Physics, Russian Academy of Sciences, ul. Ul'yanova 46, 603950 Nizhii Novgorod, Russia; e-mail: verevkin@appl.sci-nnov.ru

Received 4 April 2002
Kvantovaya Elektronika **33** (1) 76 – 80 (2003)
Translated by A.S. Seferov

2. Features of the three-level model of four-wave interactions

The diagram of the energy levels and relaxation processes analysed in this paper is shown in Fig. 1. Levels 2 and 3 correspond to an active resonance transition on which all of the waves of interest operate. Level 1 corresponds to the ground state, the parameters w_{23} and w_{32} characterise the population relaxation of the working transition, w_{13} determines the repulsive behaviour of the lower working level, and w_{21} simulates the effect of various factors [11] leading to excitation of the upper level. The equations describing the interaction of waves with such an atomic system can be written in the form (e.g., [12])

$$\begin{aligned}
&\left(\frac{\mathrm{d}}{\mathrm{d}t} - \mathrm{i}\omega_{23}\right)\rho_{32} = -\gamma_{32}\rho_{32} + \frac{V_{32}}{\mathrm{i}\hbar}\,\Delta,\\
&\frac{\mathrm{d}\rho_{23}}{\mathrm{d}t} = \frac{\mathrm{d}\rho_{32}^*}{\mathrm{d}t},\\
&\frac{\mathrm{d}\Delta}{\mathrm{d}t} = -W_1\left(\rho_{22} - \rho_{22}^{(0)}\right) - W_1^{(1)}\left(\Delta - \Delta^{(0)}\right)\\
&\qquad + \frac{2}{\mathrm{i}\hbar}\left(V_{23}\rho_{32} - \rho_{23}V_{32}\right),\\
&\frac{\mathrm{d}\rho_{22}}{\mathrm{d}t} = -W_2\left(\rho_{22} - \rho_{22}^{(0)}\right) - W_1^{(1)}\left(\Delta - \Delta^{(0)}\right)\\
&\qquad + \frac{1}{\mathrm{i}\hbar}\left(V_{23}\rho_{32} - \rho_{23}V_{32}\right),
\end{aligned} \tag{1}$$

where ρ_{mn} are the elements of the density matrix; $\Delta = r_{22} - \rho_{33}$; $\rho_{22}^{(0)}$ and $\Delta^{(0)}$ are the steady-state (in the absence of external fields) values of these quantities; $V_{23} = V_{32}^* =$

$-\mu_{23}[E_1\exp(-\mathrm{i}\omega_1 t)+E_3\exp(-\mathrm{i}\omega_3 t)]$ are the matrix elements of the interaction operator in the rotating-wave approximation; $E_1=A_1\exp(\mathrm{i}\boldsymbol{k}_1\boldsymbol{r}+\mathrm{i}\varphi_1)+A_2\exp(\mathrm{i}\boldsymbol{k}_2\boldsymbol{r}+\mathrm{i}\varphi_2)$ is the complex amplitude of the strong field formed by counterpropagating waves at the frequency ω_1; $E_3=A_3\times\exp(\mathrm{i}\boldsymbol{k}_3\boldsymbol{r})$ is the complex amplitude of a weak wave at the frequency ω_3; μ_{23} is the matrix element of the dipole operator for levels 2 and 3; $W_1=-w_{13}+2(w_{21}-w_{23}+w_{32})$; $W_1^{(1)}=w_{13}-w_{21}+2w_{23}$; $W_2=2w_{21}-w_{23}+w_{32}$; $W_2^{(1)}=-w_{21}+w_{23}$; w_{mn} are the phenomenological factors determining the rates of transitions from the state n to the state m in the absence of external fields; and γ_{32} is the decay constant of nondiagonal matrix elements for levels 3 and 2. The frequencies ω_1 and ω_3 of the considered fields are close to the resonance with the $2\leftrightarrow 3$ transition.

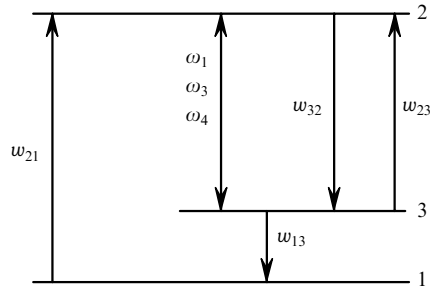

Figure 1. Three-level diagram of the medium used for the description of a four-wave interaction.

The solution to system (1) for steady-state conditions in a linear weak-field approximation shows that, if strong counterpropagating waves at the frequency ω_1 and a weak wave at ω_3 are specified, a weak wave at the frequency $\omega_4=2\omega_1-\omega_3$ is generated in the medium. If a weak wave at the frequency ω_4 exists, then a wave at the frequency $\omega_3=2\omega_1-\omega_4$ appears.

The system of algebraic equations determining the components of the density matrix elements at the above frequencies has the form

$$\begin{aligned}
&\hbar(\omega_3-\omega_{23}+\mathrm{i}\gamma_{32})\rho_{23}^{(1)}(\omega_3)-\mu_{23}E_1\Delta^{(1)}(\omega_3-\omega_1)\\
&\quad=\mu_{23}E_3\Delta^{(0)}(0),\\
&\hbar(\omega_3-2\omega_1+\omega_{23}+\mathrm{i}\gamma_{32})\rho_{32}^{(1)}(\omega_3-2\omega_1)\\
&\quad+\mu_{32}E_1^*\Delta^{(1)}(\omega_3-\omega_1)=0,\qquad(2)\\
&2\mu_{23}E_1\rho_{32}^{(1)}(\omega_3-2\omega_1)-2\mu_{32}E_1^*\rho_{23}^{(1)}(\omega_3)\\
&+\hbar[\omega_3-\omega_1+\mathrm{i}W_1\Phi_1(\omega_3-\omega_1)+\mathrm{i}W_1^{(1)}]\Delta^{(1)}(\omega_3-\omega_1)\\
&\quad=-2\mu_{23}E_3\rho_{32}^{(0)}(-\omega_1),
\end{aligned}$$

where

$$\rho_{32}^{(0)}(-\omega_1)=\rho_{23}^{(0)*}(\omega_1)=\frac{\hbar^{-1}\mu_{32}E_1^*\Delta^{(0)}(0)}{\omega_1-\omega_{23}-\mathrm{i}\gamma_{32}};$$

$$\Phi_1(\omega_3-\omega_1)=\frac{\omega_3-\omega_1+\mathrm{i}\left(W_1^{(1)}-2W_2^{(1)}\right)}{2(\omega_3-\omega_1)-\mathrm{i}(W_1-2W_2)};\ \text{and}$$

$$\Delta^{(0)}(0)=\frac{[1+(\omega_1-\omega_{23})^2\gamma_{32}^{-2}]\Delta^{(0)}}{1+(\omega_1-\omega_{23})^2\gamma_{32}^{-2}+4\hbar^{-2}\gamma_{32}^{-1}\Phi^{-1}|\mu_{32}|^2|E_1|^2}$$

is the steady-state value of Δ taking into account a saturation caused by the wave E_1 ($E_3=0$);

$$\Phi=2\,\frac{W_1W_2^{(1)}-W_1^{(1)}W_2}{W_1-2W_2};$$

and $\Delta^{(1)}(\omega_3-\omega_1)$ is the frequency component of the population difference. Using the system of Eqs (2), we find the frequency components of the elements ρ_{23} and ρ_{32} at the frequencies ω_3 and $2\omega_1-\omega_3$, respectively:

$$\begin{aligned}
\rho_{23}^{(1)}(\omega_3)&=\frac{\mu_{23}E_3\Delta^{(0)}(0)}{\hbar D(\omega_3)}\\
&\times\left[\left\{\omega_3-\omega_1+\mathrm{i}\left[W_1\Phi_1(\omega_3-\omega_1)+W_1^{(1)}\right]\right\}\right.\\
&\left.\times(\omega_3-2\omega_1+\omega_{23}+\mathrm{i}\gamma_{32})-\frac{2\hbar^{-2}|\mu_{32}|^2|E_1|^2(\omega_3-\omega_1)}{\omega_1-\omega_{23}-\mathrm{i}\gamma_{32}}\right],\\
\rho_{32}^{(1)}(\omega_3-2\omega_1)&=\frac{2\mu_{32}|\mu_{32}|^2E_1^{*2}E_3\Delta^{(0)}(0)}{\hbar^3D(\omega_3)}\\
&\times\frac{\omega_3-\omega_1+2\mathrm{i}\gamma_{32}}{\omega_1-\omega_{23}-\mathrm{i}\gamma_{32}},
\end{aligned}\qquad(3)$$

where

$$\begin{aligned}
D(\omega_3)&=\left\{\omega_3-\omega_1+\mathrm{i}\left[W_1\Phi_1(\omega_3-\omega_1)+W_1^{(1)}\right]\right\}\\
&\times(\omega_3-\omega_{23}+\mathrm{i}\gamma_{32})(\omega_3-2\omega_1+\omega_{23}+\mathrm{i}\gamma_{32})\\
&-4\hbar^{-2}|\mu_{32}|^2|E_1|^2(\omega_3-\omega_1+\mathrm{i}\gamma_{32}).
\end{aligned}$$

The obtained values $\rho_{23}^{(1)}(\omega_3)$ and $\rho_{32}^{(1)}(\omega_3-2\omega_1)$ allow us to determine the polarisation at the frequencies ω_3 and ω_4, which are the excitation sources of the corresponding waves. Expressions (3) are similar to formulas (8) from [9]. The relations obtained can be adapted to a two-level scheme by tending w_{13} to zero. In this case, the quantities Φ and $W_1\Phi_1(\omega_3-\omega_1)+W_1^{(1)}$ transform into the sum $w_{23}+w_{32}$.

Let us compare spectral and nonlinear-optical differences in the behaviour of the matrix element $\rho_{32}(\omega_3-2\omega_1)$ for a frequency-nondegenerate ($\omega_1\neq\omega_3$) four-wave interaction for two- and three-level models. The characteristics of the fourth wave $\omega_4=2\omega_1-\omega_3$ are determined, in particular, by the matrix element ρ_{32}. Consider the case of the exact resonance $\omega_1=\omega_{23}$ under the condition that $T_2=\gamma_{32}^{-1}\ll w_{32}^{-1}$, w_{23}^{-1}, w_{21}^{-1}, which is valid for the active transitions of excimer molecules. We can then select fast and slow terms dependent on ω_3 in the expression for $|\rho_{32}^{(1)}(\omega_3-2\omega_1)|$ and replace the slow terms by their values at the maximum of the transition band. This allows us to derive the analytic expression for the spectral width $\Delta\omega_{0.5}$ of the effective four-wave interaction. Taking into account that, for a two-level model, $w_{13}\ll w_{32}$, w_{23}, w_{21}, we obtain

$$\Delta\omega_{0.5}=2\sqrt{3}(w_{23}+w_{32})(1+I^{(1)}),$$

where

$$I^{(1)} = \frac{4|\mu_{32}|^2|E_1|^2}{\hbar^2\gamma_{32}(w_{23}+w_{32})}.$$

For $w_{13} \gg w_{32}$, w_{23}, w_{21}, we have

$$\Delta\omega_{0.5} = 2\sqrt{3}(w_{21}+w_{32})(1+I^{(11)}),$$

where

$$I^{(11)} = \frac{2|\mu_{32}|^2|E_1|^2}{\hbar^2\gamma_{32}(w_{21}+w_{32})}.$$

As a rule, $w_{21} < w_{32} \approx w_{23}$; therefore, the width of the interaction in the three-level model is smaller than that in the two-level model (at $I^{(1)} \approx I^{(11)}$). Fig. 2 shows the spectral dependence $|\rho_{32}^{(1)}(\omega_3 - 2\omega_1)|$ for some relations between the parameters of the transitions. Curve (*1*) corresponds virtually to a two-level model, when w_{13} is much lower than the other transition probabilities in the system. Curves (*2–4*) characterise a three-level model (w_{13} is large compared to other transition probabilities). The interaction bandwidth for curve (*2*) is approximately two times smaller than that in the two-level model. As w_{21} increases, the interaction bandwidth increases in accordance with the above approximate formula.

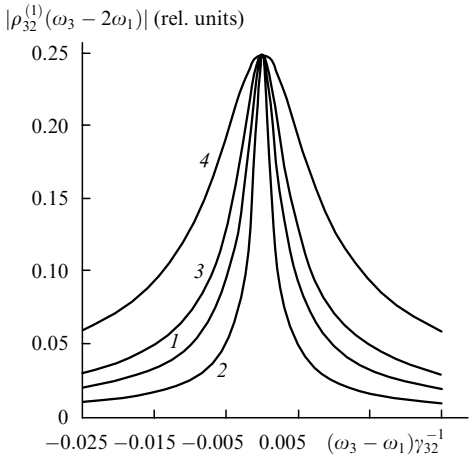

Figure 2. Spectral dependences $|\rho_{32}^{(1)}(\omega_3 - 2\omega_1)|$ in an almost two-level model at $w_{13} = 2\times10^{2.5}$ s^{-1}, $w_{21} = 10^7$ s^{-1} (*1*) and a three-level model at $w_{13} = 2\times10^{12}$ s^{-1}, $w_{21} = 10^7$ (*2*), 10^9 (*3*), and $10^{9.4}$ s^{-1} (*4*) for $w_{32} = w_{23} = 0.5\times10^9$ s^{-1}, $\gamma_{32} = 10^{12}$ s^{-1}, $\omega_1 = \omega_{23}$, and $I/I_{\rm sat} = 1$.

The presence of the third level also affects the saturation intensity, which can be determined from formulas (2):

$$I_{\rm sat} = \frac{c}{4\pi}\frac{\hbar^2\gamma_{32}\Phi}{4|\mu_{32}|^2}.$$

For the two-level model (for $w_{13} \to 0$),

$$I_{\rm sat} = \frac{c}{4\pi}\frac{\hbar^2\gamma_{32}(_{23}+_{32})}{4|\mu_{32}|^2},$$

and for the three-level model (for $w_{13} \geqslant 1/T_2$),

$$I_{\rm sat} = \frac{c}{4\pi}\frac{\hbar^2\gamma_{32}(w_{21}+w_{32})}{2|\mu_{32}|^2}.$$

At $w_{23} \simeq w_{32} \simeq w_{12}$, these saturation intensities differ by a factor of ~ 2. If $w_{21} \ll w_{32}$ and $w_{23} \approx w_{32}$, they are virtually equal for both models.

3. Nondegenerate four-wave interaction in a medium with a large gain (absorption coefficient)

The small-signal gain in an active XeCl plasma is usually $\sim e^6 - e^{15}$ per pass in an amplifier. This means that, when analysing four-wave interactions in such a medium, it is necessary to take into account changes in the amplitudes of strong waves along the medium.

The results obtained above make it possible to write equations for complex amplitudes of weak waves E_3 and E_4 and simultaneously take into account the changes in the amplitudes and phases of the strong waves. According to [9], we obtain truncated equations for the weak waves $E_j = A_j \exp(i\boldsymbol{k}_j\boldsymbol{r})$ ($j = 3, 4$):

$$ik_{3z}\frac{dA_3}{dz} = 2\frac{\alpha_3 N(\omega_3) + \alpha_3' A_1 A_2}{D'(\omega_3)}A_3$$

$$+ k_3^{(0)}\frac{2(A_1-A_2)^2N(\omega_3) - (A_1^2+A_2^2)}{D'(\omega_3)}A_4^*\exp(i\Delta k_z z), \quad (4)$$

$$-ik_{4z}\frac{dA_4^*}{dz} = 2\frac{\alpha_4^* N^*(\omega_4) + \alpha_4'^* A_1 A_2}{D'^*(\omega_4)}A_4^*$$

$$+ k_4^{(0)*}\frac{2(A_1-A_2)^2N^*(\omega_4) - (A_1^2+A_2^2)}{D'^*(\omega_4)}A_3\exp(-i\Delta k_z z). \quad (5)$$

Eqns (4) and (5) have the following notation:

$$D'(\omega_3) = \gamma_3\delta\left(1+\frac{4\Omega_0^2A_1A_2}{\delta}\right)^{1/2}\left(1+\frac{4\xi_3\Omega_0^2A_1A_2}{\gamma_3}\right)^{1/2}$$

$$\times\left[\left(1+\frac{4\Omega_0^2A_1A_2}{\delta}\right)^{1/2} + \left(1+\frac{4\xi_3\Omega_0^2A_1A_2}{\gamma_3}\right)^{1/2}\right];$$

$$N(\omega_3) = \left[\xi_3\delta\Omega_0^2A_1A_2\left(1+\frac{4\Omega_0^2A_1A_2}{\delta}\right)^{1/2}\right.$$

$$\left. - \gamma_3\Omega_0^2A_1A_2\left(1+\frac{4\xi_3\Omega_0^2A_1A_2}{\gamma_3}\right)^{1/2}\right]$$

$$\times\left\{\gamma_3\delta\left[\left(1+\frac{4\xi_3\Omega_0^2A_1A_2}{\gamma_3}\right)^{1/2} - \left(1+\frac{4\Omega_0^2A_1A_2}{\delta}\right)^{1/2}\right]\right\}^{-1};$$

$$\delta = 1 + (\omega_1-\omega_{23})^2\gamma_{32}^{-2} + \Omega_0^2(A_1-A_2)^2;$$

$$\Omega_0^2 = 4\hbar^{-2}|\mu_{32}|^2\Phi^{-1}\gamma_{32}^{-1};$$

$$\gamma_3 = \left\{(\omega_3-\omega_1)\left[W_1\Phi_1(\omega_3-\omega_1) + W_1^{(1)}\right]^{-1} + i\right\}$$

$$\times\left[(\omega_3-\omega_{23})\gamma_{32}^{-1} + i\right]\left[(\omega_3-2\omega_1+\omega_{23})\gamma_{32}^{-1} + i\right]$$

$$+ \xi_3\Omega_0^2(A_1-A_2)^2;$$

$$\xi_3 = -\Phi\left[W_1\Phi_1(\omega_3-\omega_1)+W_1^{(1)}\right]^{-1}\left[(\omega_3-\omega_1)\gamma_{32}^{-1}+\mathrm{i}\right];$$

$$\alpha_3 = 2\alpha_{03}k_3\gamma_{32}^{-1}\left[W_1\Phi_1(\omega_3-\omega_1)+W_1^{(1)}\right]^{-1}$$

$$\times[1+(\omega_1-\omega_{23})^2\gamma_{32}^{-2}]\{\omega_3-\omega_1+\mathrm{i}[W_1\Phi_1(\omega_3-\omega_1)+W_1^{(1)}]\}$$

$$\times(\omega_3-2\omega_1+\omega_{23}+\mathrm{i}\gamma_{32})+\alpha_3'(A_1-A_2)^2;$$

$$\alpha_{03} = -2\pi\hbar^{-1}k_3N_0|\mu_{32}|^2\gamma_{32}^{-1}\Delta^{(0)};$$

$$\alpha_3' = -4\alpha_{03}k_3\hbar^{-2}|\mu_{32}|^2\gamma_{32}^{-1}\left[W_1\Phi_1(\omega_3-\omega_1)+W_1^{(1)}\right]^{-1}$$

$$\times\left[1+(\omega_1-\omega_{23})^2\gamma_{32}^{-2}\right](\omega_3-\omega_1)(\omega_1-\omega_{23}-\mathrm{i}\gamma_{32})^{-1};$$

$$k_3^{(0)} = -4\alpha_{03}k_3\hbar^{-2}|\mu_{32}|^2\gamma_{32}^{-1}\left[W_1\Phi_1(\omega_3-\omega_1)+W_1^{(1)}\right]^{-1}$$

$$\times[1+(\omega_1-\omega_{23})^2\gamma_{32}^{-2}](\omega_3-\omega_1+2\mathrm{i}\gamma_{32})$$

$$\times(\omega_1-\omega_{23}+\mathrm{i}\gamma_{32})^{-1}\exp(\mathrm{i}\varphi_1+\mathrm{i}\varphi_2).$$

Here, Δk_z is the z component of the mismatch vector $\Delta\boldsymbol{k} = \boldsymbol{k}_1+\boldsymbol{k}_2-\boldsymbol{k}_3-\boldsymbol{k}_4$, and N_0 is the atomic density. The expressions for the coefficients α_4^*, $\alpha_4'^*$, $k_4^{(0)*}$, and functions $D'^*(\omega_4)$ and $N^*(\omega_4)$ are obtained when index 3 is replaced by 4 in the formulas for the corresponding coefficients and the complex conjugate values are taken. All the coefficients in (4) and (5) for the degenerate regime ($\omega_3=\omega_1$) remain unaltered regardless of the two- or three-level atomic model adopted. The only difference is the expressions for the saturation intensities. The amplitude distributions for the strong waves along their propagation direction ($A_1(z)$ and $A_2(z)$) were found from the solution to the problem of the amplification of two counterpropagating waves in the active medium.

The geometrical arrangement of the wave vectors of the interacting waves is shown in Fig. 3. All the angles are considered small for the electromagnetic field to be described by a one-dimensional wave equation. An approximate formula can be written for the z component of the mismatch vector:

$$\Delta k_z \simeq 2[|\boldsymbol{k}_3|-|\boldsymbol{k}_1|+|\boldsymbol{k}_3|\theta'(\theta''+\theta'-\theta_1)]. \qquad (6)$$

According to Fig. 3, the wave-vector components in Eqns (4) and (5) are $k_{3z}<0$ and $k_{4z}>0$.

An interesting parameter that can be found from the solution to Eqns (4) and (5) is the reflection coefficient $R = |A_3(0)/A_4^*(0)|^2$ provided that the amplitude A_3 at the exit from the active medium ($A_3(L)=0$, where L is the active-medium length). Fig. 4 presents R as a function of the intensity of the strong waves at the entrance to the active medium for various gains K_0 of the weak-signal intensity. If a theory neglecting a change in the strong waves during their propagation in the active medium is used (see formula (20) in [7]), the coefficient R tends to infinity already at $K_0 \sim \mathrm{e}^{6.7}$. If this change is taken into account, the maximum R value is ~ 20. Note that, in the first case at $K_0 \sim \mathrm{e}^8$, the dependence of R on the normalised intensity has two points at which R becomes infinitely large: at $I/I_{\mathrm{sat}} \sim 0.1$ and ~ 1. In the second case, R has only one peak at $I/I_{\mathrm{sat}} \leqslant 10^{-3}$. Such differences between the two models can be understood if we pay attention to the dependence of the gain K of the counterpropagating waves on their intensity at the entrance to the active medium (Fig. 5). In the approximation used in [7], it is assumed that this gain is independent of the waves' intensity at the entrance. However, Fig. 5 shows that, at optimal intensities of the strong waves, their gain changes by several tens of times. It is the amplification saturation effect that leads to a significant reduction in the reflection coefficient R.

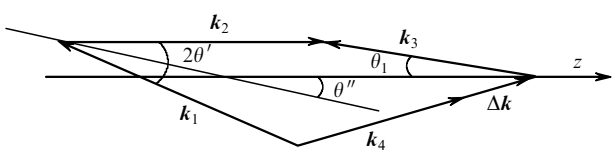

Figure 3. Diagram of the wave vectors of the interacting waves; $|\boldsymbol{k}_1| = |\boldsymbol{k}_2|$.

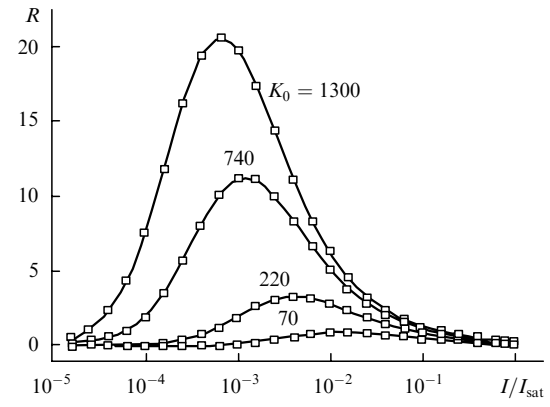

Figure 4. Coefficient of reflection R into the conjugate wave as a function of the intensity of strong waves at the entrance to the active medium for various small-signal intensity gains at $\omega_3 = \omega_1 = \omega_{23}$.

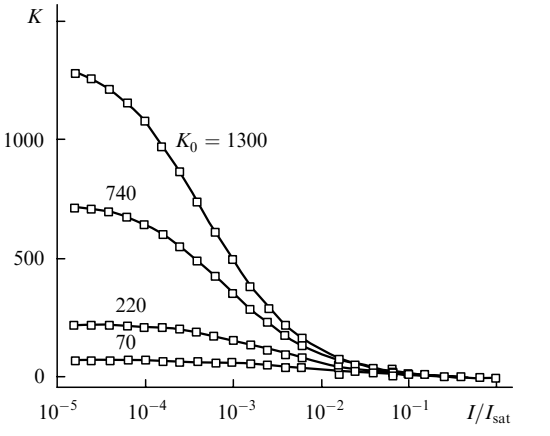

Figure 5. Intensity gain K for counterpropagating waves as a function of their intensity at the entrance to the active medium for various small-signal intensity gains at $\omega_1 = \omega_{23}$.

4. Experimental setup and reflection-coefficient measurements

A schematic of the experimental setup for investigating the four-wave interaction in an active XeCl plasma is shown in Fig. 6. A standard optical scheme for measuring the intensities of two strong (I_1 and I_2), probing (I_4), and reflected (I_3) waves is used. Its specific feature is that, in order to measure the small-signal gain, we utilised the spontaneous emission on the working transition, whose intensity was recorded by a photodetector (*7*) at a small ($\sim 1^\circ$) angle to the amplifier axis. A correlation between the spontaneous-emission intensity and the small-signal gain was preliminarily established using a single wave of the probe radiation. The experimental gain was varied between 50 and 600 through changes in the high voltage across storage capacitors and due to a mutual synchronisation of the probe radiation source with the plasma discharge in the amplifier studied.

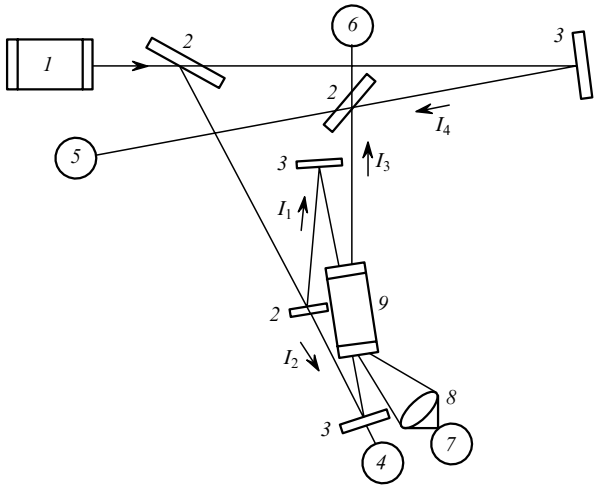

Figure 6. Schematic of the experimental setup: (*1*) narrowband master oscillator; (*2*) dielectric mirrors with a reflectivity $r = 50$ %; (*3*) dielectric mirrors with $r = 98$ %; (*4–7*) photodetectors; (*8*) focusing lens; and (*9*) active medium under study.

A two-stage XeCl laser with a diffraction-limited divergence, a pulse duration of ~ 10 ns, a spectral width of ~ 0.03 cm^{-1}, and a pulse energy of < 10 mJ served as a probe radiation source. The intensity of the strong waves was usually ~ 1 % of the saturation intensity, and the probe wave intensity was ˜10 times lower. The minimum intensity of the probe waves was determined by the sensitivity of the recording instruments. The probe wave was directed into the active medium at an angle of $\sim 10 - 30'$ to the propagation direction of the strong waves. The diameter of all the beams used in the experiment was ~ 6 mm.

Fig. 7 shows the coefficient of reflection into the conjugate wave measured as a function of the small-signal gain. Due to the short pulse duration of the probe radiation and a short time of the existence of a uniform plasma-discharge stage, the experimental conditions differ from the steady-state conditions considered theoretically. When comparing such measurements with calculations (Fig. 4), only a qualitative agreement between them can be expected. A quantitative comparison requires a narrower spectrum of the probe waves or a shorter length of the active medium (*9*) (Fig. 6). Such experiments are planned for the future.

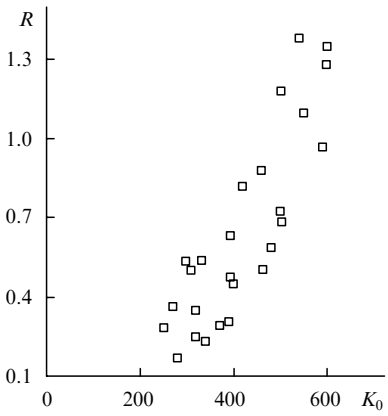

Figure 7. Experimental dependences of the coefficient of reflection R into the conjugate wave on the small-signal gain K_0.

5. Conclusions

The theoretical and experimental investigations performed have shown the possibility of obtaining a high-efficiency phase conjugation for weak signals in an active XeCl plasma. Note also that four-wave interactions in this plasma result in a spurious generation and an increase in the intensity of the amplified spontaneous emission inside the resonator of the narrow-band master oscillator and in multipass optical amplifiers.

Acknowledgements. This work was supported by the Russian Foundation for Basic Research (Grant Nos 98-02-16306 and 02-02-17639).

References

1. Yajima T., Souma H. *Phys. Rev. A*, **17** (1), 309 (1978).
2. Butylkin V.S., Kaplan A.E., Khronopulo Yu.G., Yakubovich E.I. *Rezonansnoe vzaimodeistvie sveta s veshchestvom* (Resonant Light Interaction with Matter) (Moscow: Nauka, 1977) p. 351.
3. Betin A.A., Dyatlov A.I., Kulagina S.N., Milovskii N.D., Rusov N.Yu. *Kvantovaya Elektron.*, **13**, 1975 (1986) [*Sov. J. Quantum Electron.*, **16**, 1304 (1986)].
4. Galushkin M.G., Gordon E.B., Drozdov M.S., Polyakov E.Yu. *Izv. Akad. Nauk, Ser. Fiz.*, **58** (6), 125 (1994).
5. Spiro A.G. *Opt. Spektrosk.*, **82** (3), 379 (1997).
6. Lind R.C., Steel D.G., Dunning G.J. *Opt. Eng.*, **21** (2), 190 (1982).
7. Abrams R.L., Lam J.F., Lind R.C., Steel D.G., Liao P.F., in *Optical Phase Conjugation* (New York: Acad. Press, 1983) pp 211 – 284.
8. Bodunov E.N. *Opt. Spektrosk.*, **72** (6), 1383 (1992).
9. Harter D.J., Boyd R.W. *IEEE J. Quantum Electron.*, **16** (10), 1126 (1980).
10. Mesyats G.A., Osipov V.V., Tarasenko V.F. *Impul'snye gazovye lazery* (Pulsed Gas Lasers) (Moscow: Nauka, 1991).
11. Tikhonov E.A., Shpak M.E. *Nelineinye opticheskie yavleniya v organicheskikh soedineniyakh* (Nonlinear Optical Phenomena in Organic Compounds) (Kiev: Naukova dumka, 1979) Ch. 3.
12. Klyshko D.N. *Fizicheskie osnovy kvantovoi elektroniki* (Physical Principles of Quantum Electronics) (Moscow: Nauka, 1986) Ch.3.